Bulletin of the Seismological Society of America, Vol. 108, No. 1, pp. 409–417, February 2018, doi: 10.1785/0120160319

Relationships among Various Definitions of Horizontal Spectral Accelerations in Central and Eastern North America

by Alireza Haji-Soltani and Shahram Pezeshk

Abstract A single ground-motion intensity measure, typically spectral acceleration (SA), is required as the main input in deriving empirical ground-motion prediction equations (GMPEs). Traditionally, a single horizontal orientation has been used in calculating SA for all periods. The spectrum changes with orientation, and using a single orientation to represent 2D ground motions leads to loss of useful information regarding the variation of SA with orientation. Different techniques have been proposed in the literature to combine the two horizontal components of ground motions into a scalar horizontal definition. The ratios between different definitions of the horizontal component of ground motions have been studied because of the urgent need to use multiple GMPEs combined in a logic-tree framework in the preliminary stages of performing probabilistic seismic hazard analysis, or at further stages in which the uniform hazard response spectrum is required to be converted to another spectrum for a different horizontal definition. Although the most recent studies produced similar results using different subsets of the Next Generation Attenuation-West2 Project (NGA-West2) database, it is possible that such directionality results may differ for other earthquake datasets and is region specific. The purpose of this study is to derive ratios between median values and the associated standard deviations for different definitions of the horizontal component of ground motions in central and eastern North America using a subset of the NGA-East database. The computed median ratios are similar to the ratios provided in recent studies for other regions with a shift in some period ranges with noticeable differences between the standard deviations. The results of this study fulfill the engineering requirements of considering the maximum direction elastic response spectrum for design of structures.

Introduction

Ground motions are generally recorded in three pairwise perpendicular directions: one vertical and two horizontal. A single ground-motion intensity measure, typically spectral acceleration (SA), is required as the main input in deriving empirical ground-motion prediction equations (GMPEs). A variety of GMPEs have been developed based on a single horizontal orientation of ground motion; that is, the horizontal orientation which has the larger peak ground acceleration (PGA) or the horizontal component randomly chosen (Douglas, 2003). Apparently, the spectrum changes with orientation, and using a single orientation to represent 2D ground motions leads to loss of information regarding the variation of spectrum with orientation. Alternatively, different techniques have been proposed in the literature to combine the two horizontal components of ground motions into a scalar definition. For example, the geometric mean of the acceleration response spectra for each as-recorded horizontal component of the ground motion (SA_{GMxy}, in which the GM stands for the geometric mean, and x and y stand for the two orthogonal orientations) has been traditionally preferred in deriving GMPEs (Douglas, 2003; Abrahamson *et al.*, 2008). Most of the GMPEs used by the U.S. Geological Survey (USGS) in deriving the National Seismic Hazard Maps were developed based on SA_{GMxy} (Petersen *et al.*, 2008, 2014). The advantage of SA_{GMxy} is that the data dispersion will be reduced slightly during the averaging procedure (Stewart *et al.*, 2011). However, SA_{GMxy} is variant to the orientation of the instruments. This means that if one of the sensors' orientations is aligned with the polarization direction, the response spectrum on the other sensor would be zero, which would result in a zero value for SA_{GMxy} (Boore *et al.*, 2006). The sensor orientation dependency of SA_{GMxy} is prominent in highly correlated ground motions, which regularly occurs at oscillator frequencies of 1.0 Hz and lower (Campbell and Bozorgnia, 2007). To compensate for this drawback, Boore *et al.* (2006) proposed an orientation-independent technique for calculating the geometric mean of the acceleration response spectra calculated from the rotation of the two orthogonal horizontal components of the ground motions ($SA_{GMRotDpp}$ and $SA_{GMRotIpp}$, in which the subscript Rot stands for the rotation, the subscript D signifies the period-dependent rotations, the subscript I signifies the period-independent rotations, and the subscript pp indicates the percentile). For example, $SA_{GMRotI50}$ would be the 50th percentile (or median) SA which has been used in updating the Next Generation Attenuation-West2 Project (NGA-West2) GMPEs of Abrahamson and Silva (1997), Boore *et al.* (1997), Sadigh *et al.* (1997), and Campbell and Bozorgnia (2003a,b,c, 2004) published in the Pacific Earthquake Engineering Research Center (PEER) NGA Project (Abrahamson *et al.*, 2008). Later on, Boore (2010) introduced two more orientation-independent definitions of horizontal ground motion without calculating geometric means, known as SA_{RotDpp} and SA_{RotIpp}. The NGA-West2 GMPEs (Bozorgnia *et al.*, 2012) and the NGA-East GMPEs of Darragh *et al.* (2015), Frankel (2015), Graizer (2015), Hassani *et al.* (2015), Pezeshk *et al.* (2015), Shahjouei and Pezeshk (2015), and Yenier and Atkinson (2015) in PEER 2015/4 (see Data and Resources) are developed based on SA_{RotD50}.

Engineers are required to design structures considering the maximum direction elastic response spectrum. Typically, the elastic response spectrum is obtained using GMPEs that have been developed or calibrated using different definitions of the horizontal components of recorded ground motions. To determine the response spectrum at the maximum direction, either one has to develop GMPEs based on SA in the maximum direction or because most GMPEs have been developed based on different horizontal definitions, one needs to use a set of adjustment factors to convert the obtained spectrum into maximum direction response spectrum. The reason for using the maximum direction response spectrum is to design structures that can resist possible collapse in any horizontal direction regardless of orientation. If only one component is chosen randomly, then it may underestimate forces imparted to the structure. Similarly, geometric mean cannot provide the necessary level of forces to design structures. Regardless of which directionality definition would be the most appropriate choice, the main concern will be the consistency throughout the entire process of the seismic hazard analysis, site-response analysis, and ultimately developing a design response spectrum. This would clearly ensure that the relationship between the two horizontal components of the ground motions are properly well-kept during the acceleration time-histories selection and the spectrum matching procedure in the dynamic design of structures (Baker and Cornell, 2006; Beyer and Bommer, 2006). The engineering community's preference is to use the maximum direction for structural design (National Earthquake Hazard Reduction Program [NEHRP], 2009). Therefore, it is valuable to investigate the median ratios between different definitions of the horizontal ground-motion components and their aleatory variabilities to define appropriate conversion factors.

Several researchers have studied the ratios between different definitions of the horizontal component of ground motions. Beyer and Bommer (2006) provided relationships between the median values and the standard deviation for a variety of existing horizontal-component definitions. They computed the median ratio of each definition of horizontal component with respect to the geometric mean of the two horizontal components of the ground motion. They used a subset of the NGA-West2 database (PEER, 2005, see Data and Resources) including 949 far-field and near-fault records from 103 shallow crustal earthquakes. They assumed that the ratios are only a function of response period and did not explore any dependencies of the ratios on the earthquake magnitude, the source-to-site distance, or other seismological parameters. They also declared that the ratios are not tested for stable continental regions, such as central and eastern North America (CENA).

Boore *et al.* (2006) used 3500 records from the NGA-West dataset to calculate the mean of $\ln(SA_{GMRotD50}/SA_{GMRotI50})$ and $\ln(SA_{GMRotI50}/SA_{GMxy})$. He showed that the median ratio of $SA_{GMRotD50}/SA_{GMRotI50}$ is roughly 1.0, whereas the median ratio of $SA_{GMRotI50}/SA_{GMxy}$ is slightly higher than 1.0 over a period range of 0.01–3.0 s.

Campbell and Bozorgnia (2007, 2008) provided the ratios between SA_{GMxy} and $SA_{GMRotI50}$. They showed that the median ratios are very close to unity and are constant for all periods, whereas the standard deviation increases from ~0.07 to 0.11 in natural log units. They also provided the ratios of some other horizontal definitions such as the arbitrary horizontal component, maximum horizontal component (largest peak amplitude), maximum rotated horizontal component ($SA_{RotD100}$), and strike-normal and strike-parallel horizontal components ("the peak amplitudes of the two orthogonal horizontal components after rotating them to azimuth that are normal to and parallel to the strike of the rupture plane," p. 42) with respect to SA_{GMxy}.

Watson-Lamprey and Boore (2007) provided the conversion factors from $SA_{GMRotI50}$ to $SA_{RotD100}$ and to the SA of a randomly chosen horizontal component of ground motion (SA_{Arb}, in which the subscript Arb stands for arbitrary). They used a subset of the NGA-West2 database, which included 7080 individual horizontal-component acceleration time histories recorded from 175 earthquakes. They investigated if the median ratios are highly dependent on earthquake magnitude, source-to-site distance, and a simplified radiation pattern. Their results showed that the median ratios are not significantly sensitive to the magnitude, the distance, and the radiation pattern. Also, they did not find any dependency on the most common directivity factors for the ratio of $SA_{RotD100}/SA_{GMRotI50}$.

Huang *et al.* (2008) investigated the relationships between strike-parallel, strike-normal, geometric mean, and maximum spectral demands using a subset of the NGA-West2 database, including 147 records from near-field earthquakes with moment magnitude **M** of 6.5 and greater, and rupture distances of 15 km and less. They developed scaling factors to transform $SA_{GMRotI50}$ to $SA_{RotD100}$, which ranged from 1.2 at a period of 0 to 1.3 at a period of 4.0 s, similar to the Beyer and Bommer (2006) results. They also studied the rupture directivity effects using the Somerville *et al.* (1997) rupture directivity model and showed that smaller strike-parallel demands compared with the strike-normal demands only hold at close distances (0–5 km) to the causative fault. For greater distances, there is approximately a 40%–50% probability that the strike-normal demands are equal to or fall below the strike-parallel demands. Huang *et al.* (2010) expanded the Huang *et al.* (2008) results by adding 165 pairs of western United States far-field ground motions with the moment magnitudes **M** 6.5 and greater, and the closest site-to-source distances between 30 and 50 km. They also added 63 pairs of ground-motion records from 19 earthquakes that occurred generally in CENA and provided the median ratio of $SA_{RotD100}/SA_{GMRotI50}$ for each dataset separately.

Boore (2010) used 3225 two-component time series from the NGA-West2 database to assess the ratios of $SA_{RotD50}/SA_{GMRotI50}$ and $SA_{RotI50}/SA_{GMRotI50}$. He showed that the median ratios are mostly larger than 1.0 and increase with spectral period. He also found that the ratio of $SA_{RotD100}/SA_{RotD50}$ is between unity and $\sqrt{2}$ for all periods for the unpolarized and polarized ground motions, respectively. The response spectrum of an unpolarized ground motion in all orientations is approximately identical, whereas the polarized ground motions have different numerical SA values in each orientation.

Shahi and Baker (2014) developed empirical models to compute the median ratio of $SA_{RotD100}/SA_{RotD50}$. They used more than 3000 time series from the expanded NGA-West2 database to build a multiplicative factor, which can be used to convert the SA_{RotD50} to $SA_{RotD100}$ at a desired site. They compared their results with older models and showed that the current NEHRP ratio of 1.1 at high frequencies is not appropriate and should be about 1.2 (Building Seismic Safety Council [BSSC], 2009).

Bradley and Baker (2014) studied the ground-motion directionality from the 2010–2011 Canterbury earthquake sequence recorded at 20 strong-motion stations. They examined the ratios between $SA_{RotD100}$, SA_{RotD50}, SA_{Larger} (larger value of the two as-recorded components at each period), and SA_{GMxy}. Their directionality ratio between $SA_{RotD100}$ and SA_{RotD50} was similar to Shahi and Baker (2014). They found strong polarity for rupture distances up to $R_{rup} = 30$ km and showed that complex fault ruptures show larger variability in the maximum direction orientation. They also examined the site effects on directionality ratios and found that the directionality ratios obtained for several sites somewhat differ from those calculated based on all sites over a narrow range of periods.

Although most of the above-mentioned studies produced similar results using different subsets of the NGA-West2 database (Chiou *et al.*, 2008), it is possible that such directionality results may differ for other earthquake datasets or regions with different tectonic settings. The purpose of this study is to derive ratios between the median values and between the standard deviations for different definitions of horizontal component of ground motions in CENA using a subset of the NGA-East ground-motion database (Goulet *et al.*, 2014). We focused on deriving the conversion factors to transform the median values of SA_{GMxy} and SA_{RotD50} to the median value of $SA_{RotD100}$, which is mostly required by the engineering provisions (e.g., BSSC, 2009) to design structures. These median ratios can be used along with the magnitude and distance-scaling factors when multiple GMPEs are combined in a logic-tree framework in performing probabilistic seismic hazard analysis (Bommer *et al.*, 2005). Furthermore, the provided conversion factors can be used as an approximation in converting a uniform hazard spectrum to another spectrum for a different horizontal definition of the ground motion.

Database

The dataset used to compute ratios between various horizontal definitions in this study consist of 6892 records from 48 earthquakes obtained from the NGA-East ground-motion database (Goulet *et al.*, 2014), a database that is basically different from those of earlier studies. The NGA-East database includes time series from several earthquakes recorded in the CENA region since 1988. Only the earthquakes with **M** greater than 3.5 were included to focus on ground motions that are significant from the engineering point of view. The considered CENA earthquakes are summarized in Table 1. Figure 1 shows the magnitude–distance distribution of the considered records accompanied with the associated NEHRP site classes: rock ($760 \le V_{S30} \le 1500$ m/s), soft rock ($360 \le V_{S30} < 760$ m/s), and stiff soil ($180 \le V_{S30} < 360$ m/s). The NEHRP site class E (soft-soil) sites are excluded from consideration because of their complex site-response characteristics. We performed a sensitivity test and did not find a reasonable dependency of the ratios on earthquake magnitude, distance, or style of faulting. Our sensitivity analysis is echoed in the similar earlier study by Watson-Lamprey and Boore (2007), who noted "for most engineering applications the conversion factors independent of those variables can be used."

Different Horizontal Spectral Acceleration Definitions

Different definitions of horizontal SA values which have been considered in this study are summarized in Table 2. Although it is straightforward to calculate most of the horizontal definitions, one may refer to the references provided in Table 2 for more details. As it can be observed from Table 2, three horizontal definitions represent SA values for the geometric mean combinations of orthogonal horizontal components (SA_{GMxy}, $SA_{GMRotIpp}$, and $SA_{GMRotDpp}$) and the remaining represent the SA values in a particular orientation. It should be noted that SA_{GMxy} and $SA_{LargerPGA}$ are calculated using the orientation of the as-recorded horizontal ground-motion components.

The SA/SA_{GMxy} ratios for different horizontal definitions and standard deviation of $\log(SA/SA_{GMxy})$ are illustrated in Figure 2. We have not included the median ratios of $SA_{GMRotI50}$, SA_{RotI50}, $SA_{GMRotI100}$, and $SA_{RotI100}$ with respect to SA_{GMxy} in Figure 2 because the shape of the median ratio curves depends highly on the penalty function and the period range which has been used in computing the penalty function (Boore *et al.*, 2006). The median ratios of $SA_{GMRotD50}$ and SA_{RotD50} with respect to SA_{GMxy} are close to unity up to $T = 0.1$ s. The median ratio of SA_{RotD50}/SA_{GMxy} starts increasing toward $T > 0.1$ s, whereas the median ratio of $SA_{GMRotD50}/SA_{GMxy}$ remains approximately flat for all the considered periods. The median ratio of the $SA_{GMRotD100}/SA_{GMxy}$ has a similar increasing trend with a larger ratio at shorter periods. We observe larger median ratios for the $SA_{RotD100}/SA_{GMxy}$ with a sharper increasing trend. This increasing trend after $T = 0.2$ s is due to the stronger polarization of ground-motion waves at longer periods (Beyer and Bommer, 2006). Among all the considered median ratios, the median ratio of $SA_{LargerPGA}/SA_{GMxy}$ is the only one which shows a decreasing trend with period. As it can be seen from Figure 2, the standard deviations of the logarithmic ratios of $SA_{GMRotD50}$ and SA_{RotD50}, and $SA_{GMRotD100}$ and $SA_{RotD100}$ with respect to SA_{GMxy} are below 0.05 up to $T = 0.3$ s and show a similar increasing trend with period. The standard deviations of the $\log(SA_{LargerPGA}/SA_{GMxy})$ are comparatively larger than the other horizontal definitions whereas the standard deviations of the $\log(SA_{GMRotD50}/SA_{GMxy})$ are the smallest value.

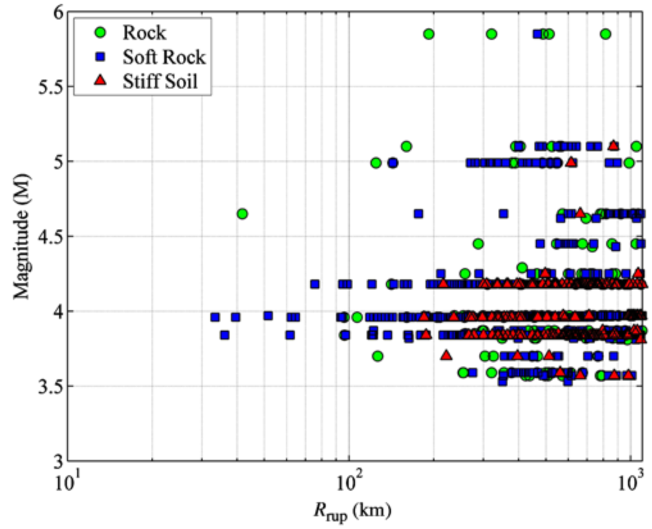

Figure 1. Magnitude–distance distribution. The color version of this figure is available only in the electronic edition.

Methodology

Among all the horizontal definitions listed in Table 2, we have only calculated the median ratios and the standard devia-

Table 1
Considered Central and Eastern North America (CENA) Earthquakes in This Study

Event Name	Date (yyyy/mm/dd)	Latitude (°)	Longitude (°)	Magnitude	Event Name	Date (yyyy/mm/dd)	Latitude (°)	Longitude (°)	Magnitude
Acadia	2006/10/03	44.35	−68.15	3.87	LacLaratelle	2002/06/05	52.85	−74.35	3.81
Arcadia	2010/11/24	35.63	−97.25	3.96	LaMalbaie	1997/10/28	47.67	−69.91	4.29
Ashtabula	2001/01/26	41.87	−80.80	3.85	LaMalbaie	2003/06/13	47.70	−70.09	3.53
AuSableForks	2002/04/20	44.51	−73.70	4.99	Laurentide	2000/07/12	47.55	−71.08	3.65
Bardwell	2003/06/06	36.87	−88.98	4.05	Lincoln	2010/02/27	35.55	−96.75	4.18
BarkLake	2003/10/12	47.01	−76.36	3.82	MilliganRdg	2005/02/10	35.75	−90.23	4.14
Blytheville	2003/04/30	35.94	−89.92	3.60	Mineral	2011/08/23	37.91	−77.98	5.74
Boyd	2002/11/03	42.77	−98.90	4.18	Mineral	2011/08/25	37.94	−77.90	3.97
Caborn	2002/06/18	37.98	−87.80	4.55	Miston	2005/06/02	36.14	−89.46	4.01
CapRouge	1997/11/06	46.80	−71.42	4.45	MtCarmel	2008/04/18	38.45	−87.89	5.30
Charleston	2002/11/11	32.40	−79.94	4.03	MtCarmel*	2008/04/18	38.48	−87.89	4.64
Charlevoix	2001/05/22	47.65	−69.92	3.60	MtCarmel	2008/04/21	38.47	−87.82	4.03
Comal	2011/10/20	28.81	−98.15	4.71	MtCarmel	2008/04/25	38.45	−87.87	3.75
CoteNord	1999/03/16	49.62	−66.34	4.43	PrairieCntr	2004/06/28	41.44	−88.94	4.18
Enola	2001/05/04	35.21	−92.19	4.37	RiviereDuLoup	2005/03/06	47.75	−69.73	4.65
FtPayne	2003/04/29	34.49	−85.63	4.62	RiviereDuLoup	2008/11/15	47.74	−69.74	3.57
Greenbrier	2011/02/28	35.27	−92.34	4.68	Saguenay	1988/11/25	48.12	−71.18	5.85
Greentown	2010/12/30	40.43	−85.89	3.85	ShadyGrove	2005/05/01	35.83	−90.15	4.25
Guy	2010/10/15	35.28	−92.32	3.86	Slaughterville	2010/10/13	35.20	−97.31	4.36
Guy	2010/11/20	35.32	−92.32	3.90	Sparks	2011/11/05	35.57	−96.70	4.73
Hawkesbury	2011/03/16	45.58	−74.55	3.59	Sparks	2011/11/06	35.54	−96.75	5.68
Jefferson	2003/12/09	37.77	−78.10	4.25	Sullivan	2011/06/07	38.12	−90.93	3.89
Jones	2010/01/15	35.59	−97.26	3.84	Thurso	2006/02/25	45.65	−75.23	3.70
Kipawa	2000/01/01	46.84	−78.93	4.62	ValDesBois	2010/06/23	45.90	−75.50	5.10

*Aftershock.

tions for the ones that are essentially needed by the engineering provisions (e.g., BSSC, 2009), which are $\mathrm{SA_{RotD100}}/\mathrm{SA}_{\mathrm{GM}xy}$ and $\mathrm{SA_{RotD100}}/\mathrm{SA_{RotD50}}$. The most commonly used GMPEs developed for the CENA sites are either based on $\mathrm{SA}_{\mathrm{GM}xy}$ or $\mathrm{SA_{RotD50}}$, whereas the engineering community is more interested in the maximum direction (e.g., $\mathrm{SA_{RotD100}}$) for design of structures. The calculated median ratios can be used as multiplicative conversion factors. We also calculated the median ratio of $\mathrm{SA_{RotD100}}/\mathrm{SA_{GMRotI50}}$ to compare our results with the recent models in terms of using a ground-motion database from a region with alternative tectonic settings and geological characteristics.

Generally, the SA of a horizontal component of ground motion with an arbitrary orientation is assumed to be lognormally distributed (Abrahamson, 1998; Beyer and Bommer, 2006; Jayaram and Baker, 2008). Typically, GMPEs include two terms: (1) the logarithmic mean value of the ground-motion measure (median value) and (2) the variation from the logarithmic mean as

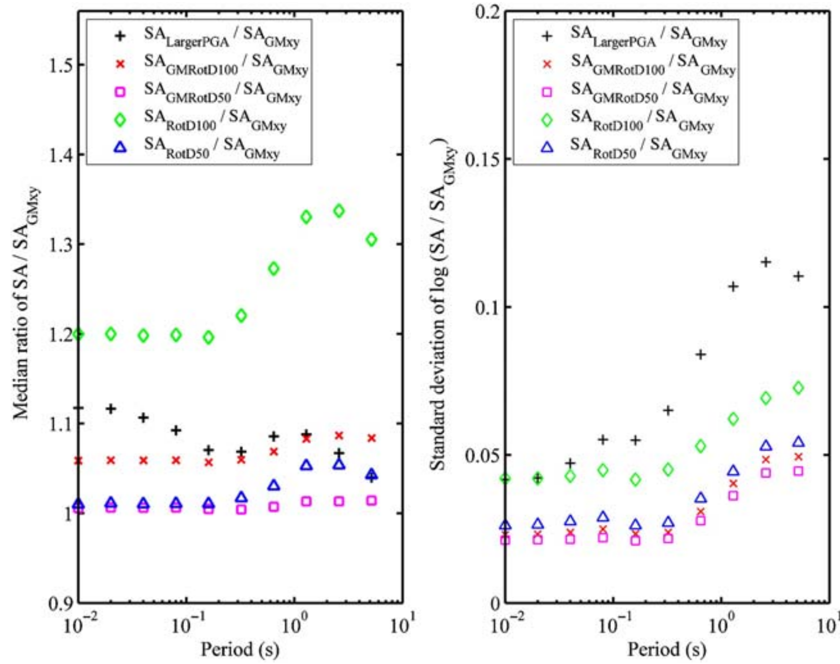

Figure 2. (Left) Median ratios of horizontal spectral ordinates for different definitions of the horizontal components of ground motion with respect to $\mathrm{SA}_{\mathrm{GM}xy}$. (Right) Standard deviation of logarithmic ratios of horizontal spectral ordinates for different definitions of the horizontal components of ground motion with respect to $\mathrm{SA}_{\mathrm{GM}xy}$. SA, spectral acceleration. The color version of this figure is available only in the electronic edition.

$$\log(Y) = \mu_{\log Y} + \sigma_{\log Y}, \tag{1}$$

in which Y is the ground-motion intensity measure, $\mu_{\log Y}$ is the mean value of the logarithm of the ground-motion intensity measure, and $\sigma_{\log Y}$ is the associated aleatory variability. Assuming SA as the ground-motion intensity measure, equation (1) can be rewritten as

$$\log(\mathrm{SA}_i) = \widehat{\mathrm{SA}}_i + \sigma_{\log \mathrm{SA}_i}, \tag{2}$$

in which $\widehat{\mathrm{SA}}_i$ corresponds to the median value of SA. On the other hand, the median ratios can be calculated to define conversion factors which can be used as a multiplicative factor to convert the median value of a host horizontal SA definition ($\widehat{\mathrm{SA}}_{\mathrm{host}}$) coming from a GMPE to a target horizontal definition ($\widehat{\mathrm{SA}}_{\mathrm{target}}$) as

$$\widehat{\mathrm{SA}}_{\mathrm{target}} = \left(\frac{\mathrm{SA_{target}}}{\mathrm{SA_{host}}}\right)_{\mathrm{median}} \times \widehat{\mathrm{SA}}_{\mathrm{host}}, \tag{3}$$

Table 2

Horizontal Spectral Acceleration (SA) Definitions Considered in This Study

Symbol	Horizontal Definition of Spectral Acceleration	Reference
$\mathrm{SA}_{\mathrm{GM}xy}$	Geometric mean of response spectra of x and y components	—
$\mathrm{SA_{LargerPGA}}$	The horizontal orientation which has the larger peak ground acceleration (PGA)	—
$\mathrm{SA_{GMRotIpp}}$	ppth percentile of the geometric mean of the acceleration response spectra calculated from the period-independent rotation of the two orthogonal horizontal components of the ground motions. The $\mathrm{SA_{GMRotI50}}$ and $\mathrm{SA_{GMRotI100}}$ are typically considered as the 50th and 100th (i.e., maximum) percentiles, respectively.	Boore *et al.* (2006)
$\mathrm{SA_{GMRotDpp}}$	ppth percentile of the geometric mean of the acceleration response spectra calculated from the period-dependent rotation of the two orthogonal horizontal components of the ground motions. The $\mathrm{SA_{GMRotD50}}$ and $\mathrm{SA_{GMRotD100}}$ are typically considered as the 50th and 100th (i.e., maximum) percentiles, respectively.	Boore *et al.* (2006)
$\mathrm{SA_{RotIpp}}$	ppth percentile of the acceleration response spectra calculated from the period-independent rotation of the two orthogonal horizontal components of the ground motions. The $\mathrm{SA_{RotI50}}$ and $\mathrm{SA_{RotI100}}$ are typically considered as the 50th and 100th (i.e., maximum) percentiles, respectively.	Boore (2010)
$\mathrm{SA_{RotDpp}}$	ppth percentile of the acceleration response spectra calculated from the period-dependent rotation of the two orthogonal horizontal components of the ground motions. The $\mathrm{SA_{RotD50}}$ and $\mathrm{SA_{RotD100}}$ are typically considered as the 50th and 100th (i.e., maximum) percentiles, respectively.	Boore (2010)

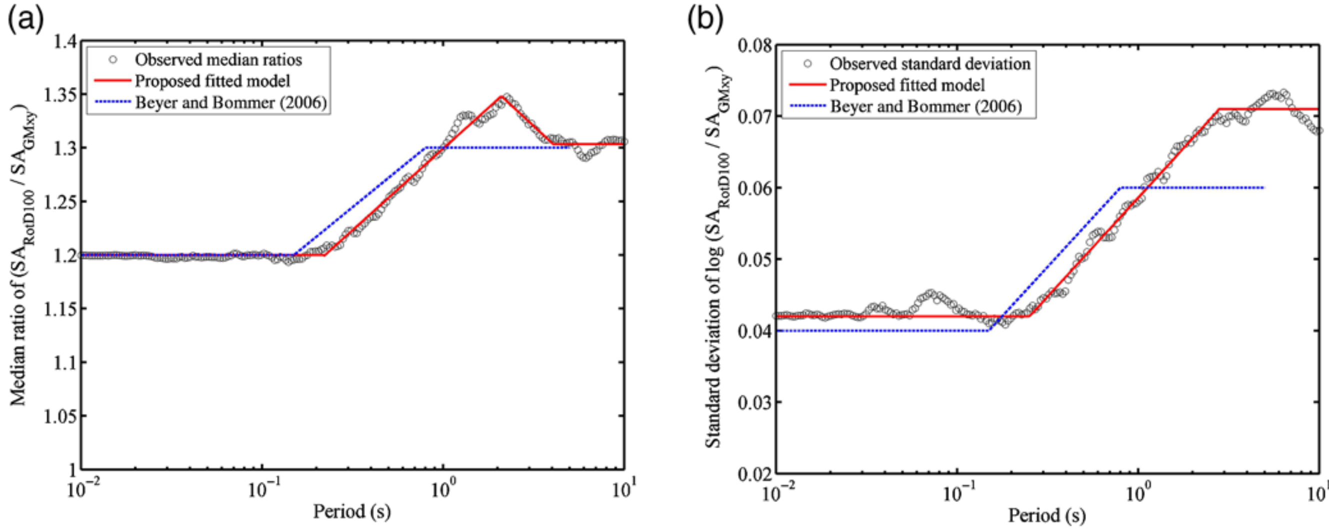

Figure 3. (a) Median ratio of $SA_{RotD100}/SA_{GMxy}$ observed as a function of period. (b) Standard deviation of $\log(SA_{RotD100}/SA_{GMxy})$ observed as a function of period. The Beyer and Bommer (2006) model is also plotted for comparison. The color version of this figure is available only in the electronic edition.

in which $(SA_{target}/SA_{host})_{median}$ represents the expected value of the $\log(SA_{target}/SA_{host})$. It is worth mentioning that we did not use a mixed-effects analysis, because it is likely that any process that produced an event-specific change in the ground-motion intensity measures would be canceled out when the ratios were computed. According to results of Shahi and Baker (2014), the intraevent standard deviations from a mixed-effects analysis were very small compared with the interevent standard deviations.

Conversion Factors and Comparison

The obtained ratios are compared with the median and the standard deviation of the Beyer and Bommer (2006) and Shahi and Baker (2014) models in Figures 3 and 4, respectively. Figure 3 illustrates the obtained median ratio of $SA_{RotD100}/SA_{GMxy}$ and the standard deviation of the $\log(SA_{RotD100}/SA_{GMxy})$, which is generally in good agreement with the Beyer and Bommer (2006) model for both the median ratio and the standard deviation for short periods of up to $T = 0.15$ s. The median ratios follow similar increasing trend with a roughly parallel slope as to the Beyer and Bommer (2006) model for longer periods with a noticeable shift toward longer periods. The main difference occurs at $T = 0.8$ s in which the Beyer and Bommer (2006) model becomes flat for longer periods (up to $T = 5.0$ s) while the obtained ratios keep increasing up to $T = 2.2$ s. However, the obtained median ratios decrease in the period range of $2.2 < T < 4.0$ s and finally becomes flat. The obtained ratio of $\log(SA_{RotD100}/SA_{GMxy})$ is higher than the Beyer and Bommer (2006) model in the longer periods. Figure 4 shows the median ratio of $SA_{RotD100}/SA_{RotD50}$ and the standard deviation of the $\log(SA_{RotD100}/SA_{RotD50})$ obtained from this study and the results of the Shahi and Baker (2014) model. As it can be seen, the median ratios are in good agreement with the Shahi and Baker (2014) model for the periods of $T < 0.1$ s with a roughly similar increasing trend with the period. Interestingly, we see a noticeable shift toward larger spectral periods. Also, the obtained median ratios cross the results of Shahi and Baker (2014) at a period of ~1.0 s. An interesting observation is the difference between the obtained standard deviations and the results of Shahi and Baker (2014). The standard deviation in the Shahi and Baker (2014) model is a fixed value for all periods with two exceptions for 0.5 and 0.75 s at which the standard deviations are increased. The obtained standard deviation from this study remains flat up to the period of $T = 0.3$ s followed by a mild jump up to $T = 2.5$ s. The obtained ratios start around $T = 6.0$ s followed by a decreasing trend toward $T = 10.0$ s.

We propose a simple piecewise linear model in logarithmic space for both the median ratio and the standard deviation of the logarithmic ratios as

$$R = \begin{cases} c_1 + \alpha_1 \log(T), & T < T_1 \\ c_2 + \alpha_2 \log(T), & T_1 \le T < T_2 \\ c_3 + \alpha_3 \log(T), & T_2 \le T < T_3 \\ c_4, & T \ge T_3, \end{cases} \quad (4)$$

in which R is the ratio and c_1–c_4 and α_1–α_3 are the regression coefficients that are provided in Table 3. The hinged points are different for the observed standard deviations.

It should be noted that the calculated median ratio of $SA_{GMRotI50}/SA_{GMxy}$ is very close to 1.0 similar to the Beyer and Bommer (2006) model. To make a final comparison between the obtained median ratios and recent published models, the median ratio of $SA_{RotD100}/SA_{GMRotI50}$ is plotted in Figure 5. The results of the Watson-Lamprey and Boore (2007), the Beyer and Bommer (2006), the Campbell and

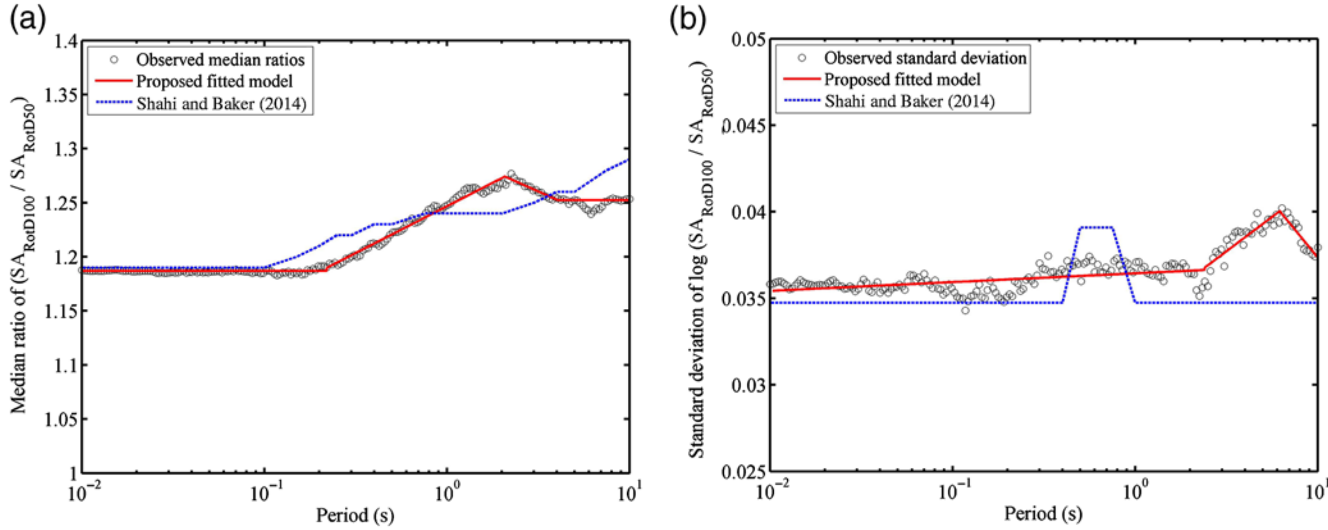

Figure 4. (a) Median ratio of $SA_{RotD100}/SA_{RotD50}$ observed as a function of period. (b) Standard deviation of $\log(SA_{RotD100}/SA_{RotD50})$ observed as a function of period. The Shahi and Baker (2014) model is also plotted for comparison. The color version of this figure is available only in the electronic edition.

Bozorgnia (2007), the Huang *et al.* (2010), and the NEHRP (BSSC, 2009) models are also included for comparison. As it can be seen from Figure 5, the median ratios of this study are smaller than the ones provided by Huang *et al.* (2010) for CENA. Most of the models are in general agreement, in terms of the magnitude of the median ratios and an increasing trend with spectral period, except for the median ratios provided in the NEHRP (BSSC, 2009) provisions.

The proposed ratios of $SA_{RotD100}/SA_{GMRotI50}$ in NEHRP are calculated as the ratio of observed $SA_{RotD100}$ values in recorded ground motions to the $SA_{GMRotI50}$ values predicted by a ground-motion prediction model. Although the NEHRP recommended ratios could be used effectively to adjust ground-motion models, it would eliminate the benefits of statistical computations, such as the mixed-effects regressions used in developing a ground-motion prediction model (Shahi and Baker, 2014). Modeling the median ratio of $SA_{RotD100}/SA_{GMRotI50}$ using the ratio of observed $SA_{RotD100}$ value to the observed $SA_{GMRotI50}$ value would save the statistical efforts used in developing ground-motion models and would provide us with a better estimation of $SA_{RotD100}$ for future probable earthquakes.

Summary and Conclusions

A subset of the NGA-East database (Goulet *et al.*, 2014) has been used to calculate the median ratios and the ratios of standard deviations between different horizontal definitions of SA in CENA. The ratios between various definitions of horizontal SA values were calculated and compared with the existing models. Such comparisons are insightful in the sense that most of such studies have mainly used the NGA-West2 database. Therefore, this study highlights the possibility that such median ratios may depend on the study region.

Simple piecewise linear equations are developed for $SA_{RotD100}/SA_{GMxy}$ and $SA_{RotD100}/SA_{RotD50}$ based on the assumption that the horizontal SA values are lognormally distributed. The computed median ratios and the standard deviation were compared with the Beyer and Bommer (2006) and Shahi and Baker (2014) models. The observed median ratio of $SA_{RotD100}/SA_{GMxy}$ follows a similar increasing trend as compared with the Beyer and Bommer (2006) model with a noticeable shift toward longer periods. A similar increasing trend with spectral period was also seen for the median ratio of $SA_{RotD100}/SA_{RotD50}$ compared with the

Table 3
Coefficients of the Proposed Model for the Median Ratio and the Standard Deviation

	Regression Coefficients							Period (s)		
R	c_1	c_2	c_3	c_4	α_1	α_2	α_3	T_1	T_2	T_3
$SA_{RotD100}/SA_{GMxy}$	1.200	1.299	1.398	1.303	0.0	0.152	−0.156	0.22	2.20	4.00
$SA_{RotD100}/SA_{RotD50}$	1.187	1.247	1.298	1.252	0.0	0.086	−0.075	0.22	2.20	4.00
$\sigma_{\log(SA_{RotD100}/SA_{GMxy})}$	0.042	0.059	0.071	—	0.0	0.028	0.000	0.25	2.80	10.00
$\sigma_{\log(SA_{RotD100}/SA_{RotD50})}$	0.035	0.037	0.050	—	0.001	0.008	−0.013	2.50	6.00	10.00

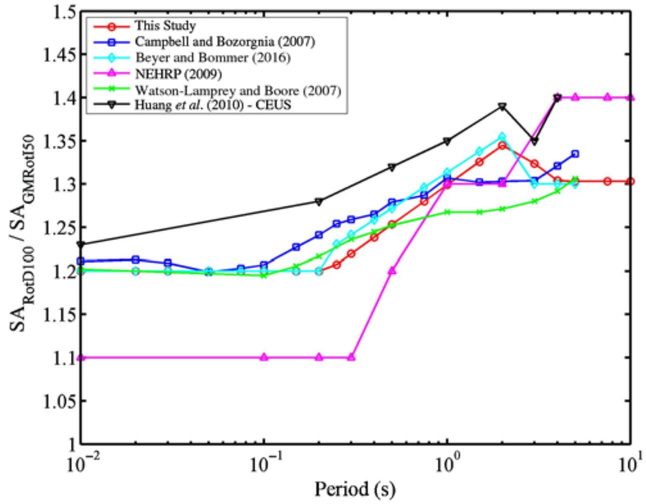

Figure 5. Median ratio of $SA_{RotD100}/SA_{GMRotI50}$ observed as a function of period. NEHRP, National Earthquake Hazard Reduction Program; CEUS, central and eastern United States. The color version of this figure is available only in the electronic edition.

Shahi and Baker (2014) results. However, the obtained standard deviations are smaller. We also explored the median ratio of $SA_{RotD100}/SA_{GMRotI50}$ and compared our results with the recent models. The obtained median ratios were smaller compared with the Huang *et al.* (2010) results.

Data and Resources

The Pacific Earthquake Engineering Research Center (PEER) Next Generation Attenuation-East Project (NGA-East) database was searched using http://peer.berkeley.edu/publications/peer_reports/reports_2015/reports_2015.html (last accessed June 2016) and https://ngawest2.berkeley.edu/ (last accessed March 2016).

Acknowledgments

The authors would like to thank Yousef Bozorgnia and Chris Cramer for providing the Next Generation Attenuation-East Project (NGA-East) ground-motion database. The authors also would like to thank the anonymous reviewer for the constructive comments.

References

Abrahamson, N. A. (1998). Statistical properties of peak ground accelerations recorded by the SMART 1 array, *Bull. Seismol. Soc. Am.* **78,** 26–41.

Abrahamson, N. A., and W. J. Silva (1997). Empirical response spectral attenuation relations for shallow crustal earthquakes, *Seismol. Res. Lett.* **68,** 94–127.

Abrahamson, N. A, G. M. Atkinson, D. M. Boore, Y. Bozorgnia, K. W. Campbell, B. Chiou, I. M. Idriss, W. J. Silva, and R. R. Youngs (2008). Comparisons of the NGA ground-motion relations, *Earthq. Spectra* **24,** 45–66.

Baker, J. W., and C. A. Cornell (2006). Which spectral acceleration are you using? *Earthq. Spectra* **22,** 293–312.

Beyer, K., and J. J. Bommer (2006). Relationships between median values and between aleatory variabilities for different definitions of the horizontal component of motion, *Bull. Seismol. Soc. Am.* **96,** 1512–1522.

Bommer, J. J., F. Scherbaum, H. Bungum, F. Cotton, F. Sabetta, and N. A. Abrahamson (2005). On the use of logic trees for ground-motion prediction equations in seismic-hazard analysis, *Bull. Seismol. Soc. Am.* **95,** 377–389.

Boore, D. M. (2010). Orientation-independent, nongeometric-mean measures of seismic intensity from two horizontal components of motion, *Bull. Seismol. Soc. Am.* **100,** 1830–1835.

Boore, D. M., W. B. Joyner, and T. E. Fumal (1997). Equations for estimating horizontal response spectra and peak acceleration from western North American earthquakes: A summary of recent work, *Seismol. Res. Lett.* **68,** 128–153.

Boore, D. M., J. Watson-Lamprey, and N. A. Abrahamson (2006). Orientation-independent measures of ground motion, *Bull. Seismol. Soc. Am.* **96,** 1502–1511.

Bozorgnia, Y., N. A. Abrahamson, K. Campbell, B. Rowshandel, and T. Shantz (2012). NGA-West2: A comprehensive research program to update ground motion prediction equations for shallow crustal earthquakes in active tectonic regions, *Proc. of the 15th World Conf. on Earthquake Engineering*, Lisbon, Portugal, 6 pp.

Bradley, B. A., and J. W. Baker (2014). Ground motion directionality in the 2010–2011 Canterbury earthquakes, *Earthq. Eng. Struct. Dynam.* **44,** 371–384.

Building Seismic Safety Council (BSSC) (2009). NEHRP Recommended Seismic Provisions for New Buildings and Other Structures (FEMA P-750), Report prepared for the Federal Emergency Management Agency (FEMA), National Institute of Building Sciences (2009 Edition), Washington, D.C.

Campbell, K. W., and Y. Bozorgnia (2003a). Updated near-source ground motion (attenuation) relations for the horizontal and vertical components of peak ground acceleration and acceleration response spectra, *Bull. Seismol. Soc. Am.* **93,** 314–331.

Campbell, K. W., and Y. Bozorgnia (2003b). Erratum to "Updated near-source ground-motion (attenuation) relations for the horizontal and vertical components of peak ground acceleration and acceleration response spectra", *Bull. Seismol. Soc. Am.* **93,** 1413.

Campbell, K. W., and Y. Bozorgnia (2003c). Erratum to "Updated near-source ground-motion (attenuation) relations for the horizontal and vertical components of peak ground acceleration and acceleration response spectra," *Bull. Seismol. Soc. Am.* **93,** 1872.

Campbell, K. W., and Y. Bozorgnia (2004). Erratum to "Updated near-source ground-motion (attenuation) relations for the horizontal and vertical components of peak ground acceleration and acceleration response spectra", *Bull. Seismol. Soc. Am.* **94,** 2417.

Campbell, K. W., and Y. Bozorgnia (2007). Campbell–Bozorgnia NGA ground motion relations for the geometric mean horizontal component of peak and spectral ground motion parameters, *PEER Report 2007/02*, Pacific Earthquake Engineering Research Center, Berkeley, California, 238

Campbell, K. W., and Y. Bozorgnia (2008). NGA ground motion model for the geometric mean horizontal component of PGA, PGV, PGD and 5% damped linear-elastic response spectra for periods ranging from 0.01 and 10.0 s, *Earthq. Spectra* **24,** 139–171.

Chiou, B., R. Darragh, N. Gregor, and W. J. Silva (2008). NGA project strong-motion database, *Earthq. Spectra* **24,** 23–44.

Douglas, J. (2003). Earthquake ground motion estimation using strong-motion records: A review of equations for the estimation of peak ground acceleration and response spectra ordinates, *Earth Sci. Rev.* **61,** 43–104.

Goulet, C. A., T. Kishida, T. D. Ancheta, C. H. Cramer, R. B. Darragh, W. J. Silva, Y. M. A. Hashash, J. Harmon, J. P. Stewart, K. E. Wooddell, *et al.* (2014). PEER NGA-East database, *PEER Report 2014/17*, Pacific Earthquake Engineering Research Center, Berkeley, California.

Huang, Y., A. Whittaker, and N. Luco (2008). Maximum spectral demands in the near-fault region, *Earthq. Spectra* **24,** 319–341.

Huang, Y., A. Whittaker, and N. Luco (2010). Establishing maximum spectral demand for performance-based earthquake engineering: Collaborative research with the University at Buffalo and the USGS, *U.S. Geol. Surv. Tech. Rept.*, USGS Award Number 08HQGR0017, Reston, Virginia.

Jayaram, N., and J. W. Baker (2008). Statistical tests of the joint distribution of spectral acceleration values, *Bull. Seismol. Soc. Am.* **98,** 2231–2243.

National Earthquake Hazards Reduction Program [NEHRP] (2009). NEHRP Recommended Seismic Provisions for New Buildings and Other Structures., *Part 1, Provisions*, National Earthquake Hazards Reduction Program, Washington, D.C., 373 pp.

Petersen, M. D., A. D. Frankel, S. C. Harmsen, C. S. Mueller, K. M. Haller, R. L. Wheeler, R. L. Wesson, Y. Zeng, O. S. Boyd, D. M. Perkins, *et al.* (2008). Documentation for the 2008 update of the United States national seismic hazard maps, *U.S. Geol. Surv. Open-File Rept. 2008–1128*, 128 pp.

Petersen, M. D., M. P. Moschetti, P. M. Powers, C. S. Mueller, K. M. Haller, A. D. Frankel, Y. Zeng, S. Rezaeian, S. C. Harmsen, O. S. Boyd, *et al.* (2014). Documentation for the 2014 update of the United States national seismic hazard maps, *U.S. Geol. Surv. Open-File Rept. 2014–1091*, 243 pp.

Sadigh, K., C.-Y. Chang, J. A. Egan, F. Makdisi, and R. R. Youngs (1997). Attenuation relationships for shallow crustal earthquakes based on California strong motion data, *Seismol. Res. Lett.* **68,** 180–189.

Shahi, S. K., and J. W. Baker (2014). NGA-West2 models for ground-motion directionality, *Earthq. Spectra* **30,** 1285–1300.

Somerville, P. G., N. F. Smith, R. E. Graves, and N. A. Abrahamson (1997). Modification of empirical strong ground motion attenuation relations to include the amplitude and duration effects of rupture directivity, *Seismol. Res. Lett.* **68,** 199–222.

Stewart, J. P., N. A. Abrahamson, G. M. Atkinson, J. Baker, D. M. Boore, Y. Bozorgnia, H. W. Campbell, C. D. Comartin, I. M. Idriss, M. Lew, *et al.* (2011). Representation of bi-directional ground motions for design spectra in building codes, *Earthq. Spectra* **27,** 927–937.

Watson-Lamprey, J., and D. M. Boore (2007). Beyond Sa_{GMRotI}: Conversion to Sa_{Arb}, Sa_{SN}, and Sa_{MaxRot}, *Bull. Seismol. Soc. Am.* **97,** 1511–1524.

Mueser Rutledge Consulting Engineers
14 Penn Plaza, 225 West 34th Street
New York, New York 10122
ahaji-soltani@mrce.com
(A.H.-S.)

Department of Civil Engineering
The University of Memphis
Engineering Science Building, Room 104A
Memphis, Tennessee 38152
spezeshk@memphis.edu
(S.P.)

Manuscript received 19 October 2016;
Published Online 12 December 2017